

High Magnetic Field Annealing Dependent the Morphology and Microstructure of Nanocrystalline Co/Ni Bilayered Films

Donggang Li^{1,2}, Alexandra Levesque², Qiang Wang^{1,3}
Agnieszka Franczak², Chun Wu¹, Jean-Paul Chopart² and Jicheng He¹

Abstract: Co/Ni bilayered films were prepared on ITO glass by electrodeposition assisted with a magnetic field up to 0.5T aligned parallel to the electrode surface. The effect of a high magnetic field annealing up to 12T on morphology and microstructure of the post-deposited films was investigated by field emission scanning electronic microscopy (FE-SEM), X-ray diffraction (XRD) and atomic force microscopy (AFM). Grain shape and grain boundary in the Co/Ni morphology were modified dramatically when the high magnetic field was applied during the annealing process. Magnetic anisotropy appeared in the films due to the preferential orientation of fcc-CoNi alloy in comparison with a weaker orientation of hcp-Co. High magnetic field annealing favored to form a more homogeneous surface with smaller grain size and lower roughness, compared with the annealed samples obtained in the absence of magnetic field. The influencing mechanisms of high magnetic field annealing on the microstructure evolution in the Co/Ni electrodeposits are interpreted in terms of the overlapping effects: diffusion, recrystallization, grain growth and magnetic domains.

Keywords: Thin Film; Electrodeposition; High magnetic fields annealing; Atomic force microscopy; Diffusion

¹ Key Laboratory of Electromagnetic Processing of Materials (Ministry of Education), Northeastern University, Shenyang, 110004, China

² LACM-DTI, Université de Reims Champagne-Ardenne, B.P. 1039, 51687 Reims Cedex 2, France

³ Corresponding author. Key Laboratory of Electromagnetic Processing of Materials (Ministry of Education), Northeastern University, No.3-11 Wenhua Road, Heping District, Shenyang, Liaoning Province, 110004, P.R.China Tel: +86-24-83681726, Fax: +86-24-83681758, E-mail address: wangq@mail.neu.edu.cn

1 Introduction

Electrodeposited nanocrystalline magnetic films have received considerable interest in the fields of data storage devices and microelectromechanical systems (MEMS) [Baghbanan et al. (2004)], since the microstructure of the film can be easily controlled on a large scale during the electrochemical processing in the comparison with a physical vapor deposition. It is well known that the physical properties of the electrodeposits strongly depend on morphology and microstructure, as reported in recent papers [Cavallotti et al. (2003); Tian et al. (2011)]. Numerous studies have been devoted to improve surface morphology and microstructure, i.e. reducing the grain size and the roughness, by magnetohydrodynamic effect (MHD), which is induced by superimposing an external magnetic field [Koza et al. (2010); Georgescu and Daub (2006); Krause et al. (2005)] during the electrodeposition process. However, the non-equilibrium state of as-electrodeposited nanocrystalline layers provides a strong thermodynamic potential for microstructural transformation. That means that the benefit effect of magneto-electrodeposition on a nanocrystalline film can be completely consumed by a thermal exposure at relatively low temperature [Hibbard et al. (2002)]. Magnetic field annealing has been confirmed to be useful for tailoring the microstructure of as-deposited nanocrystalline films for their widespread uses [Li et al. (2010)]. Markou et al. (2010) obtained a high degree (001) texture in $L1_0$ CoPt films by annealing Co/Pt bilayers in a perpendicular magnetic field of 1kOe. The advancement of superconducting technology has opened unique aspects for heat treatment in a high magnetic field. Up to date, few applications of high magnetic field (over 10T) during annealing process [Li et al. (2004)] proved it to be a promising method to control the preferential crystallographic orientation of deposited magnetic film. Though there is no doubt that a high magnetic field annealing plays an important role on grain growth, inter-diffusion [Liu et al. (2010); Li et al. (2009, 2008)], and recrystallization processes, which in turn will influence the microstructural variation of nanocrystalline film, the dependences of grain shape, grain size, roughness, and texture of electrodeposited films on the magnetic field parameters during post annealing are still unclear. In this study, we investigate the effect of post high magnetic field annealing up to 12T on Co/Ni bilayered film obtained by electrodeposition assisted with or without a 0.5T magnetic field.

2 Experimental

Nanocrystalline bilayered films were electrodeposited on ITO (1000nm thickness)/glass (1cm²) with structure of ITO glass/Ni/Co from two cells step by step. One cell contained the electrolyte of nickel sulphate 0.6M, boric acid 0.4M, and pH was

adjusted to 2.7 at 30°. The electrolyte in the other cell consisted of cobalt sulphate 0.6M, boric acid 0.4M, at 50°, pH = 4.7. The counter electrode was a rectangular Pt plate of $1 \times 2\text{cm}$, placed parallel to the working electrode. Chronopotentiometry method with a current density of 10 mA/cm^2 was performed for 6 minutes in Ni^{2+} cell, and 4 minutes in Co^{2+} cell respectively. A water-cooled electromagnet was used to produce a magnetic field of 0.5T. The magnetic field was superimposed parallel to the working electrode during the electrodeposition processing of Co film. Two series of electrodeposits were denoted 0T- B_{ed} and 0.5T- B_{ed} .

The two series of as-deposited films were heat treated at 673K for 4h under a protective atmosphere of high purity argon in a vertical furnace, which was placed inside a super-conducting magnet of up to 12T, and then cooled down to room temperature. The direction of the external magnetic field is in perpendicular to the surface of the films, and the applied magnetic flux density during the annealing process was 0T, 6T, and 12T, respectively.

Field emission scanning electronic microscopy (FE-SEM, SUPRA 35, Japan) was used to detect the surface morphology of the Co/Ni films. The topography and the roughness were investigated by the AFM (NTEGRA AURA, NT-MDT, Russia). Each sample was measured in areas of $10\mu\text{m} \times 10\mu\text{m}$ for three times at different positions of the film to obtain the average grain size and roughness of the surface. For the characterization of the films microstructure, Grazing Incidence X-Ray Diffraction (GI-XRD, Ultima IV, Japan) measurements were performed using the $\text{CuK}\alpha$ radiation (40kV, 40mA, $\lambda = 1.54$). X-ray Photoelectron Spectroscopy (XPS) measurement (ESCALAB250, Thermo VG Company, USA) was done to analysis the distribution of Co and Ni along the cross-section of the samples, by which the thickness of Co layer can also be estimated as about 1200 nm.

3 Results and discussion

The FE-SEM images in Fig. 1 show the surface morphology of annealed Co/Ni films under high magnetic fields of 0, 6, 12T. By comparing the Fig. 1(a1-a3) and Fig. 1 (b2-b3), it can be seen that the application of high magnetic field annealing played a similar role on the morphological evolution in the both series: 0T- B_{ed} and 0.5T- B_{ed} , although there is a obvious difference between the two series, which were annealed at the same 6T magnetic field condition. It is generally considered that the effects of a weak magnetic field (B_{ed}) on the morphology of electrodeposits were almost fully consumed by an annealing processing for a long time. The films after post-annealed under 0T magnetic field present a blurred irregular grain shape with a mass of velour-like deposits on the grain boundary. With the increase of the applied magnetic field, not only the grain shape and grain boundary become clear to form polyhedral grains, but also the grain size decreases with the disappear of

the velour-like deposits.

As it is well known, for magnetic and paramagnetic materials, magnetic field will induce a pulling force due to the magnetization [Coey and Hinds (2001); Tang et al. (2011)], which force is favored for the separation of grains. In the meantime, an introduction of the magnetization energy during the magnetic field annealing results in the decrease of diffusion activation energy, which will improve the diffusion of the congregated deposits on the grain boundary. This is a possible reason for the grain boundary becoming clear after post-magnetic field annealing. Another most likely reason for the disappear of velour-like product, which is estimated to be Co-oxides formed at the grain boundaries, is that the application of high magnetic fields during annealing process is favor for the reduction of oxides, but the mechanism needs further investigation.

On the other hand, we should also take into account the effect of the magnetic field annealing on recrystallization process and grain boundary migration (GBM) in the films. If magnetic field annealing plays a retarded effect on the recrystallization process as reported by Refs. [Martikainen and Lindroos (1981); Xu et al. (2000)] or a beneficial effects on GBM due to magnetic ordering as reported by Molodov et al. (2006), the grain size of the film after post-magnetic annealing should be larger than the case of annealing without a magnetic field. However, no such effects of magnetic annealing on the electrodeposited film were observed in our experiments, since we found that the grain size of the film annealed under a high magnetic field seemed smaller than that of the annealed film under a no-field condition.

In order to quantitatively analyze the effects of high magnetic fields on the roughness and the grain size of the bilayered film, AFM top view ($10 \times 10 \mu m^2$) and three-dimensional AFM image of the surface topography of nanocrystalline films annealed at different magnetic flux densities ($B_{annealing}$) are shown in Fig. 2. The grain shape of the films is similar for the two series samples annealed under magnetic flux densities of 12T, therefore we only provide the AFM images of 0.5T- B_{ed} series here. After no-field annealed, there are some ellipsoidal grains imbedding in the spherical grain matrix as seen in Fig 2 (a). While annealing in a magnetic field of 12T, most of grains are spherical, even some grains connect each other to form a chain-like structure (Fig 2 (c)).

To characterize the grain size and the surface roughness, the average values were calculated using standard software (Table 1). For 0T- B_{ed} series, the application of 6T magnetic field during annealing process does not affect the grain size, but leads to a decrease of surface roughness. The grain size of the films goes through minimum under the influence of a 12T magnetic field annealing. On the other hand, in case of 0.5T- B_{ed} series, 6T magnetic field annealing is enough to decrease the average grain size of the film from 140 nm to 100 nm.

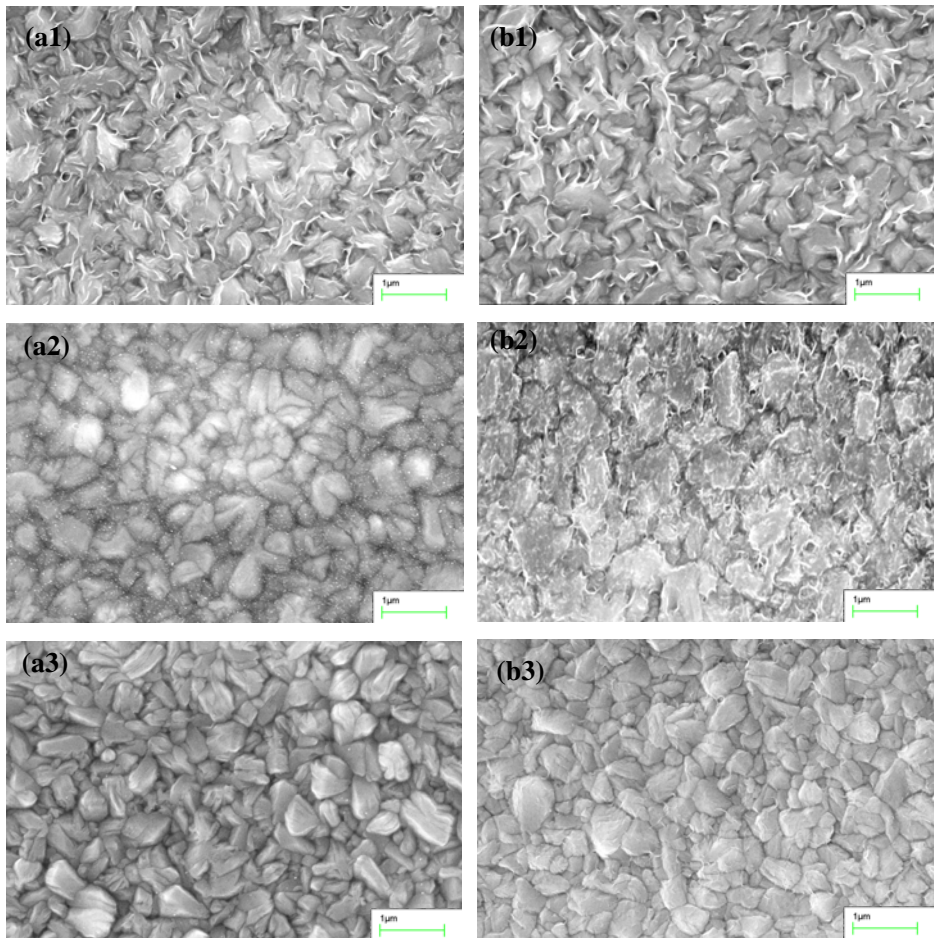


Figure 1: FE-SEM images of 0T-B_{ed} series Co/Ni film annealed under different magnetic fields (a1) 0T, (a2) 6T, (a3) 12T; and 0.5T-B_{ed} series annealed under (b1) 0T, (b2) 6T, (b3) 12T.

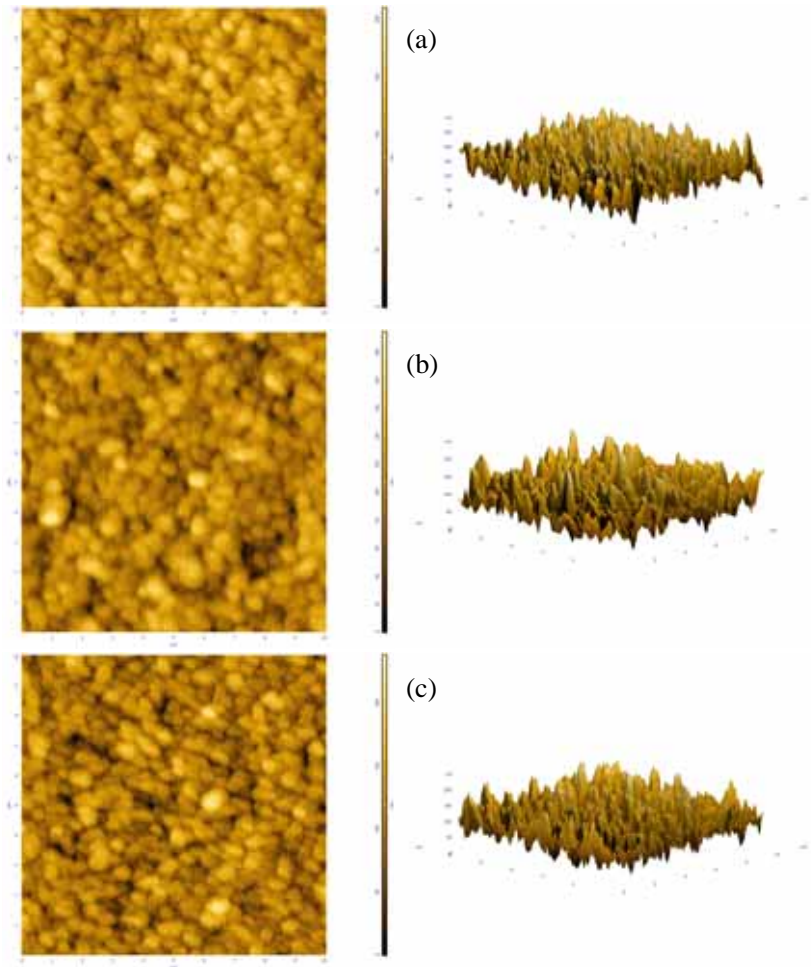


Figure 2: AFM images showing the morphology and roughness of 0.5T- B_{ed} series Co/Ni films annealed under different magnetic fields (a) 0T, (b) 6T, (c) 12T

Table 1: Dependence of the average grain size and the average roughness of the two series films on the magnetic flux density of the applied magnetic field annealing.

Series	$B_{annealing}$	Grain size (nm)	Roughness (nm)
0T- B_{ed}	0T	127±5	29±1.9
	6T	128±3	23±1.8
	12T	114±3	25±0.9
0.5T- B_{ed}	0T	140±6	28±1.5
	6T	100±3	22±1.2
	12T	104±4	24±1.6

The same magnetic annealing conditions inducing different results between the two series indicate that the influence of a weak magnetic field on the electrodeposition process can be conserved in a certain extent after post-annealing process. As to the alternation of grain size during magnetic field annealing is not in a general correlation with that of surface roughness, some researchers [Hu and Wu (2003)] also showed that a decrease of grain size was not necessarily corresponding to a decrease in the surface roughness.

According to the results in Table 1, AFM investigations show that smaller grains and lower roughness are formed during annealing in the presence of a magnetic field comparing with the case of annealing without magnetic field. This phenomenon origins from an accelerative effect of the high magnetic fields annealing on the inter-diffusion between Co and Ni films. The initial as-deposited Co film on the surface consists of 20-50nm sized grains, which distributed non-uniform with a large number of agglomerate as shown in figure 3. For a given set of annealing conditions, the nanocrystalline matrix consumed by grain growth, the mean grain size continues to increase. At the meantime, inter-diffusion behavior happens between the Co and the Ni films, which results in Co atoms diffuse into the Ni matrix to form Co-Ni alloy. The application of high magnetic fields during annealing process improved the inter-diffusion behavior according to the conclusions in Ref. [Liu et al. (2010)] and [Zhao et al. (2006)]. The experiment evidence of this improved inter-diffusion distance by magnetic field from 920nm (0T) to 1330nm (12T) was obtained by XPS analysis along cross-section of the samples. Larger volume fraction of Co-Ni nanocrystalline alloy is formed, smaller is the mean grain size. It is attributed to the crystallographic texture of Co-Ni alloy in $\alpha(fcc)$ phase comparing with $\epsilon(hcp)$ -Co, which will be discussed in details in the next section. Another possible explanation for the results in this study is the effect of field annealing on the magnetic domains. The magnetic domains tend to be directional ordering due to magnetization under magnetic annealing, which results in the decrease of the

distance between domain walls, as in turn may be responsible for the smaller grain size.

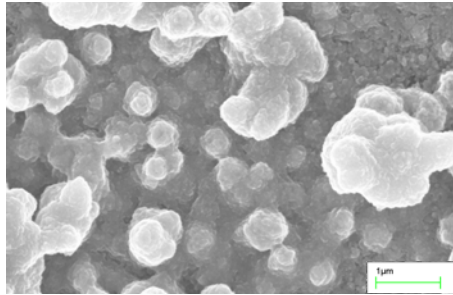


Figure 3: FE-SEM image of the as-deposited Co/Ni film (0T- B_{ed} series) before annealing

Fig. 4 presents XRD patterns for 0.5T- B_{ed} series Co/Ni films in the post-magnetic annealing state with magnetic field of 0, 6, and 12T (Note: for the 0T- B_{ed} series annealed under a high magnetic field showing the similar XRD patterns as the 0.5T- B_{ed} series). It can be seen that all the peaks of hcp-Co and fcc-Ni have been detected, but only one peak (220) of fcc-CoNi have been measured because of the alloying process. The diffraction peak (111) shifts to slightly higher diffraction angles in case of magnetic flux density of 6T. One reason for the shift is most probably because of the internal stress. Some researchers [Markou et al. (2010)] found the magnetic field annealing can change the internal stress state of films. This behavior can also be rationalized as another reason: more Co atoms are incorporated into the Ni lattice under the moderate magnetic field annealing resulting in a transition from Ni-like microstructural evolution to Co-like microstructural evolution [Tian et al. (2011)].

Since the mean grain size D calculated by Scherrer's formula $D = \frac{k\lambda}{\beta \cos \theta}$, is in inverse ratio to β , where β is the full width at half maximum (FWHM) [Culity (1978)]. Here, we list the width and the position of the peaks in Table 2. It can be seen from the data that the width of peaks mostly increases with the increasing of magnetic flux density. That also means the grain size decreased with the magnetic flux density. The change of grain size D is in the same trend as the results obtained from AFM.

There is a general trend in the increase of fcc-CoNi peak (220) and the decreasing of hcp-Co peak (110) with increasing magnetic flux density during annealing process, as can be seen in the amplified zone of Fig. 4 at the angular position from $2\theta = 75^\circ$ to 77° . A higher volume fraction of CoNi alloy in a higher magnetic field

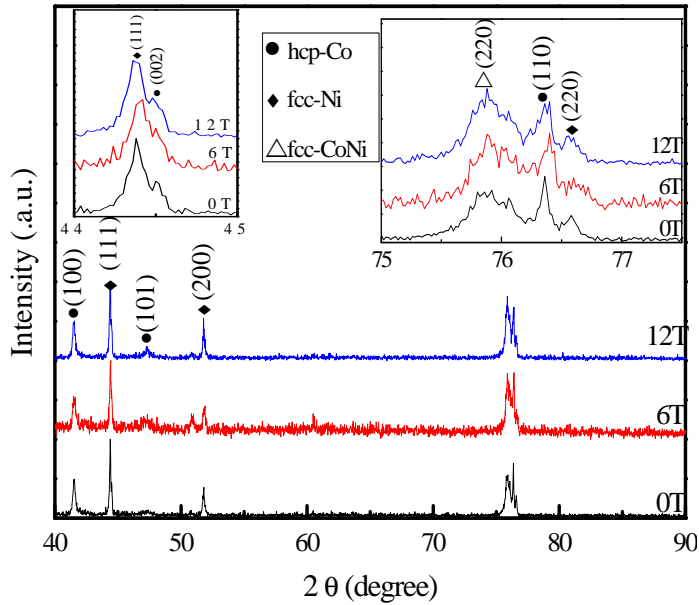


Figure 4: XRD patterns of 0.5T- B_{ed} series Co/Ni films annealed under magnetic field of $B_{annealing} = 0T, 6T$ and $12T$.

Table 2: The width and position of the peaks under different magnetic annealing conditions

$B_{annealing}$ (T)			0	6	12
FCC-Ni	(111)	2θ ($^{\circ}$)	44.44 ± 0.005	44.36 ± 0.011	44.42 ± 0.014
		FWHM	0.180 ± 0.002	0.183 ± 0.005	0.182 ± 0.004
	(200)	2θ ($^{\circ}$)	51.84 ± 0.020	51.78 ± 0.012	51.84 ± 0.011
		FWHM	0.157 ± 0.003	0.165 ± 0.006	0.160 ± 0.002
	(220)	2θ ($^{\circ}$)	76.64 ± 0.081	76.56 ± 0.014	76.62 ± 0.024
		FWHM	0.148 ± 0.008	0.161 ± 0.004	0.160 ± 0.007
HCP-Co	(100)	2θ ($^{\circ}$)	41.54 ± 0.004	41.46 ± 0.013	41.54 ± 0.007
		FWHM	0.184 ± 0.002	0.234 ± 0.003	0.225 ± 0.009
	(110)	2θ ($^{\circ}$)	76.40 ± 0.021	76.34 ± 0.022	76.40 ± 0.007
		FWHM	0.222 ± 0.008	0.261 ± 0.010	0.256 ± 0.014
FCC- CoNi	(220)	2θ ($^{\circ}$)	75.90 ± 0.081	75.82 ± 0.032	75.90 ± 0.006
		FWHM	0.364 ± 0.010	0.365 ± 0.042	0.360 ± 0.029

was conclude not only from the increase of (200)CoNi compared to the (100) Co shown in Table 3, but also from the increase of diffusion zone according to the XPS composition analysis.

Table 3: The dependence of intensity (I) ratio of the three peaks on the magnetic flux density during annealing process. In the table, Value = $I_{fcc-CoNi} / (I_{fcc-CoNi} + I_{hcp-Co} + I_{fcc-Ni}) \times 100\%$

$B_{annealing}$ (T)	fcc-CoNi (220)	hcp-Co (110)	fcc-Ni (220)
0	35.86%	45.52%	18.62%
6	40.53%	41.05%	18.42%
12	42.07%	39.80%	18.13%

The magnetism of the films in a magnetic field is favored for the transformation of $\epsilon(hcp)$ structure to a more energetically stable $\alpha(fcc)$ structure. The application of high magnetic field annealing induces a $\epsilon(hcp) \rightarrow \alpha(fcc)$ phase transformation, which may account in the increase of thermal stability of the bilayered films [Hibbard et al. (2006)].

4 Conclusions

Uniform nanocrystalline Co/Ni bilayered films were produced by the electrodeposition assisted with a 0.5T weak magnetic field. Magnetic fields annealing of up to 12T were selected in this study in order to investigate the high magnetic field effects on the evolution of morphology and microstructure of the films. A 0.5T weak magnetic field parallel to the electrode induces modification of the deposits leading changes in the grain size during magnetic field annealing. Grain shape in the Co/Ni morphology was modified with the grain boundary becoming clearer if a high magnetic field was applied during the annealing process. Atomic force microscopy investigations show that smaller grains and lower roughness are formed during annealing in the presence of a magnetic field comparing to the case of annealing without magnetic field. With increasing magnetic flux density during annealing process, the transformation from $\epsilon(hcp)$ to $\alpha(fcc)$ can be seen by the reduction of the ϵ -peak intensity, and the increase in that of α -peak. Overlapping effects of the high magnetic field annealing on diffusion, grain growth, alloying, and phase transformation have been discussed to interpret the experimental results.

Acknowledgement: The authors would like to thank Dr. Piotr Zabinski of AGH University of Science and Technology, Poland, for his contributions. This work was financially supported by the National Natural Science Foundation of

China (Grant Nos. 51061130557, 51101032, 51101034), the Fundamental Research Funds for the Central Universities (Grant No. N090209001), Agence Nationale de la Recherche France (Programme COMAGNET, Grant No. 2010-INTB-903-01) and MATERIALIA.

References

- Baghbanan, M.; Erb, U.; Palumbo, G.** (2004): In: S. M. Mukhopadhyay, S. Seal, N. Dahotre, A. Agarwal, J. E. Smugeresky, N. Moody (Eds.), *Surface and Interfaces in Nanostructured Materials and Trends in LIGA, Miniaturization and Nanoscale Materials*, The Minerals, Metals and Materials Society, Warrendale, PA, pp. 307-315.
- Cavallotti, P.L.; Vincenzo, A.; Bestetti, M.; Franz, S.** (2003): *Surf. Coat. Technol.* 76, 169-170.
- Coey, J.M.D.; Hinds, G.** (2001): *J. Alloy. Compd.* 326, 238-245.
- Culity, B. D.** (1978): *Elements of X-ray Diffraction*, 2nd edition, Addison Wesley Publishing Company, Inc, London.
- Georgescu, V.; Daub, M.** (2006): *Surf. Sci.* 60, 4195-4199.
- Hibbard et al.** (2002): *Mater. Sci. Forum.* 386-388, 387-396.
- Hibbard, G. D.; Aust, K. T.; Erb, U.** (2006): *Mater. Sci. Eng. A* 433, 195-202.
- Hu, C.-C.; Wu, C.-M.** (2003): *Surf. Coat. Technol.* 176, 75-83.
- Koza, J.A.; Karnbach, F.; Uhlemann, M.; McCord, J.; Mickel, C.; Gebert, A.; Baunack, S.; Schultz, L.** (2010): *Electrochim. Acta.* 55, 819-831.
- Krause, A.; Hamann, C.; Uhlemann, M.; Gebert, A.; Schultz, L.** (2005): *J. Magn. Magn. Mater.* 290-291 261-264.
- Li, D.S.; Garmestani, H.; Yan, Shi-shen; Elkawni, M.; Bacaltchuk, M.B.; Schneider-Muntau, H. J.; Liu, J.P.; Saha, S.; Barnard, J.A.** (2004): *J. Magn. Magn. Mater.* 281, 272-275.
- Li, D.; Wang, Q.; Li, G.; Lv, X.; Nakajima, K.; He, J.** (2008): *Mater. Sci. Eng. A* 495, 244-248.
- Li, D.; Wang, Q.; Liu, T.; Li, G.; He, J.** (2009): *Mater. Chem. Phys.* 117, 504-510.
- Li, Y.B.; Lou, Y.F.; Zhang, L.R.; Ma, B.; Bai, J.M.; Wei, F.L.** (2010): *J. Magn. Magn. Mater.* 322, 3789-3791.
- Liu, T.; Li, D.; Wang, Q.; Wang, K.; Xu, Z.; He, J.** (2010): *J. Appl. Phys.* 107, 103542 (1-3).

Markou, A.; Panagiotopoulos, I.; Bakas, T. (2010): *J. Magn. Magn. Mater.* 322, L61-L63.

Martikainen, H. O.; Lindroos, V. K. (1981): *Scand. J. Metall.* 10(1), 3-9.

Molodov, D. A.; Bhaumik, S.; Molodova, X.; Gottstein, X. (2006): *Scripta Mater.* 54(12), 2161-2164.

Tang, X.; Dai, J.; Zhu, X.; Song, W.; Sun, Y. (2011): *J. Alloy. Compd.* 509, 4748-4753.

Tian, L.; Xu, J.; Qiang, C. (2011): *Appl. Surf. Sci.* 257, 4689-4694.

Xu, Y.; Ohtsuka, Y.; Anak, K. (2000): *Trans. Mater. Res. Soc. Japan.* 25(1), 501-508.

Zhao, J.; Yang, P.; Zhu, F.; Cheng, C. (2006): *Scripta Mater.* 54 (6), 1077-1080.